Spin-orbit maximally discordant mixed states

D. G. Braga,[1,2,*] I. Fonseca,[1,2,†] W. F. Balthazar,[3,4,‡] M. S. Sarandy,[2,§] and J. A. O. Huguenin[1,2,¶]

[1]*Instituto de Ciências Exatas, Universidade Federal Fluminense, 27213-145 Volta Redonda, Rio de Janeiro, Brazil*

[2]*Instituto de Física, Universidade Federal Fluminense, Avenida General Milton Tavares de Souza s/n, Gragoatá, 24210-346 Niterói, Rio de Janeiro, Brazil*

[3]*International Iberian Nanotechnology Laboratory (INL), Avenida Mestre José Veiga, 4715-330 Braga, Portugal*

[4]*Instituto Federal do Rio de Janeiro, 27213-100 Volta Redonda, Rio de Janeiro, Brazil*

(Received 27 July 2022; accepted 18 November 2022; published 2 December 2022)

We introduce a proposal to prepare spin-obit maximally discordant mixed states by a linear optical circuit, with quantum bits (qubits) encoded in the polarization and transverse mode degrees of freedom of photons. In particular, we discuss how to prepare nonbalanced spin-orbit entangled states, applying this technique to obtain maximally discordant mixed states. We present a simulation of the optical circuit by using the Jones matrix formalism. We performed a study of entanglement, classical, and quantum correlations. The results show excellent agreement with the underlying theory and open an alternative experimental approach for addressing quantum correlations in optical setups.

DOI: 10.1103/PhysRevA.106.062403

I. INTRODUCTION

Quantum correlations are essential for the realization of quantum information tasks, with entanglement being their main resource [1]. In addition to entanglement, other (classical and quantum) correlations may play an important role in quantum protocols, such as quantum discord (QD) [2,3]. QD characterizes quantumness through the inability of a quantum state to be kept undisturbed by a nonselective measurement. QD has provided tools in several distinct scenarios, e.g., quantum spin models [4] critical quantum systems [5], quantum metrology [6], environment-induced sudden transitions [7], and multiqubit systems [8]. In photonic systems, QD has been measured in two-photon states, exploring linear optical setups [9].

In the context of QD, quantum-correlated states inherently present classical correlations. The total correlation, as provided by the mutual information, is typically divided into a quantum contribution and a classical counterpart. A natural question is then how to maximize the quantum contribution, as measured by QD, for a fixed amount of classical correlation. This maximization leads to the so-called maximally discordant mixed state (MDMS) [10]. For a pure state, it is well known that a MDMS is also a maximally entangled state, i.e., a Bell state. However, for mixed states, an unbalanced Bell state can be used to construct a MDMS. The generation of the MDMS of two qubits in the absence of quantum entanglement has been recently proposed by using two dissipative schemes, which are based on the interaction between four-level atoms and strongly lossy optical cavities [11].

From an architecture point of view, optical systems are reliable sources of entanglement [12], with qubits easily encoded in the degrees of freedom (DoF) of light. As examples of the use of DoF of light in optical systems to realize quantum information protocols, we can mention the implementation of quantum gates [13], quantum computing protocols [14], teleportation [15], and quantum cryptography [16]. Moreover, an efficient and scalable protocol for quantum computing by using linear optical elements and projective measurements in single-photon qubits has been proposed by Knill, Laflamme, and Milburn [17], yielding an intense field of research [18–20]. On the other hand, the encoding of qubits in polarization and first-order Hermite-Gaussian (HG) modes has given rise to the so-called spin-orbit modes. In turn, the classical-quantum analogy of an intense laser beam allowed for the implementation of quantum protocols with linear optical circuits for spin-orbit modes associated with intense laser beams that emulate single-photon experiments. A remarkable example was the topological phase predicted in the evolution of a pair of entangled qubits, which has been realized in this scenario [21]. Further results include experiments for bipartite systems showing violation of quantum inequalities by spin-orbit maximally nonseparable modes, such as Bell's inequality [22,23] and contextuality [24,25]. By adding path DoF to polarization and transverse modes, a tripartite system can be emulated and Mermin's inequality can be shown to be violated [26]. Such an approach has been successfully employed and has demonstrated the power of spin-orbit modes in quantum information tasks, with applications in the experimental study of environment-induced entanglement [27], quantum cryptography [28], and quantum gates [29–31].

Concerning QD, it appears in the scenario of spin-orbit modes in the proposal of an optical circuit to prepare spin-orbit X states, where QD has been derived for different classes

*danielbraga@id.uff.br
†igorrf@id.uff.br
‡wagner.blthzr@gmail.com
§msarandy@id.uff.br
¶jose_huguenin@id.uff.br

of states [32]. However, the MDMS has not been explicitly considered. In this work we present a proposal to prepare the MDMS by using spin-orbit modes in linear optical circuits. We then evaluate QD for the states resulting from the simulation of the circuit. The paper is organized as follows. In Sec. II, we present the theoretical background. We present the MDMS and the QD analysis. In Sec. III, we present in detail the linear optical circuit proposed for the preparation of the MDMS by using spin-orbit modes. Section IV is devoted to presenting the results of numerical simulation of the optical circuit by means of the Jones formalism. Finally, in Sec. V, conclusions are discussed.

II. QD AND MDMS

Let us begin by reviewing the theoretical approach to compute QD and the definition of the MDMS. Here, we used the definition of entropic QD, following the steps developed in Refs. [33,34]. In classical information theory, the uncertainty about a random variable A, which can assume the values a with the corresponding probability p_a, is provided by the Shannon's entropy $H(A) = -\sum_a p_a \log_2 p_a$. The joint uncertainty about two random variables A and B is $H(AB) = -\sum_{a,b} p_{a,b} \log_2 p_{a,b}$, with $p_{a,b}$ being the joint probability distribution. The total amount of correlation between A and B is given by the difference in the uncertainty about A before and after the variable B is known, namely, $\mathcal{J}(A:B) = H(A) - H(A|B)$, where $H(A|B) = -\sum_{a,b} p_{a,b} \log_2 p_{a|b}$ is the conditional entropy, with $p_{a|b}$ being the probability for $A = a$ given that $B = b$. From Bayes rule, $p_{a|b} = p_{a,b}/p_b$. Then, we can rewrite $\mathcal{J}(A:B)$ in the equivalent form $\mathcal{I}(A:B) = H(A) + H(B) - H(AB)$.

For the quantum case, we consider a bipartite system AB described by a composite density operator ρ. Then, the total amount of correlation between the two subsystems A and B described by local density operators ρ_A and ρ_B, respectively, is given by the quantum mutual information

$$I_m(\rho) = S(\rho_A) + S(\rho_B) - S(\rho), \tag{1}$$

where $S(\rho) = -\mathrm{Tr}[\rho \log_2 \rho]$ is the von Neumann entropy. We can also generalize $\mathcal{J}(A:B)$ to the quantum realm by considering a measurement over subsystem B, with measurement operators denoted by $\{B_k\}$. The composite state ρ then collapses to ρ_k with probability p_k. The state after the measurement ρ_k and the probability p_k is given by

$$\rho_k = \frac{1}{p_k}(I \otimes B_k)\rho(I \otimes B_k), \tag{2}$$

where

$$p_k = \mathrm{Tr}[\rho(I \otimes B_k)], \tag{3}$$

with

$$B_k = V \Pi_k V^\dagger \tag{4}$$

and

$$\Pi_k = |k\rangle\langle k| \tag{5}$$

denoting a projector in the computational basis, so $k = 0$ and 1, and $V \in \mathrm{SU}(2)$. Notice we are here restricting ourselves to projective orthogonal measurements. The measurement-based mutual information $J(\rho|\{B_k\})$ is then

$$J(\rho|\{B_k\}) = S(\rho_A) - S(\rho|B_k), \tag{6}$$

with the measurement-based conditional entropy reading $S(\rho|B_k) = \sum_k p_k S(\rho_k)$. By optimizing over the least-disturbing measurement basis, we define the classical correlation $C(\rho)$ as [2,35]

$$\begin{aligned} C(\rho) &= \max_{\{B_k\}} J(\rho|\{B_k\}) \\ &= S(\rho_A) - \min_{\{B_k\}} \sum_k p_k S(\rho_k). \end{aligned} \tag{7}$$

Oppositely to the classical case, the quantities $I_m(\rho)$ and $C(\rho)$ are generally distinct in the quantum scenario. The difference between $I_m(\rho)$ and $C(\rho)$ is the QD

$$Q(\rho) = I_m(\rho) - C(\rho). \tag{8}$$

In order to explicitly compute $Q(\rho)$, we can parametrize the unitary V, from Eq. (4), as

$$V = |\Psi\rangle\langle\Psi|, \tag{9}$$

where $|\Psi\rangle = \cos(\frac{\theta}{2})|0\rangle + \sin(\frac{\theta}{2})e^{i\phi}|1\rangle$. QD can then be explicitly obtained by performing an optimization over the angles θ and ϕ [34].

In order to build a MDMS, we have to maximize the amount of QD when compared with its classical correlation. A suitable strategy in this direction is to sacrifice some amount of entanglement to optimize QD. As show in Ref. [10], this can be achieved by the family of states

$$\begin{aligned} \rho^{\mathrm{MDMS}} = \epsilon|\Phi^+(p)\rangle\langle\Phi^+(p)| + (1-\epsilon)[m|01\rangle\langle 01| \\ + (1-m)|10\rangle\langle 10|], \end{aligned} \tag{10}$$

where

$$|\Phi^+(p)\rangle = \sqrt{p}|00\rangle + \sqrt{1-p}|11\rangle \tag{11}$$

is a partial (unbalanced) Bell state. For $p = \frac{1}{2}$, we recover a maximally entangled Bell state. If we set the value $m = 1$, Eq. (10) is reduced to a (p, ϵ) family of rank-2 states:

$$\rho^{(\mathrm{R2})} = \epsilon|\Phi^+(p)\rangle\langle\Phi^+(p)| + (1-\epsilon)|01\rangle\langle 01|. \tag{12}$$

On the other hand, for $p = \frac{1}{2}$, Eq. (10) yields a (m, ϵ) family of rank-3 states:

$$\begin{aligned} \rho^{(\mathrm{R3})} = \epsilon|\Phi^+\rangle\langle\Phi^+| + (1-\epsilon)[m|01\rangle\langle 01| \\ + (1-m)|10\rangle\langle 10|]. \end{aligned} \tag{13}$$

Equation (13) provides rank-3 states for different choices of parameters. A first rank-3 subset is $m \in [0, 1]$ and $\epsilon \in [0, \frac{1}{3}]$. A second rank-3 subset is given by $m = 1/2$ and $\epsilon \in [1/3, 0.385]$. Equation (13) can also provide rank-2 states by taking ϵ in the interval $\epsilon \in [0.408, 1]$.

III. SPIN-ORBIT MAXIMALLY DISCORDANT MIXED STATES

A spin-orbit mode is described by polarization and transverse mode DoF. The polarization of light is defined as the oscillation direction of the electric magnetic field. The circular polarization ($\sigma_\pm$) is associated with the intrinsic

angular momentum of the photon (spin). The transverse modes are solutions of Helmholtz's paraxial equation and are responsible, for example, for the transverse shape of a laser beam. For a Cartesian coordinate system, the solutions are the well-known Hermite-Gauss [$\mathrm{HG}_{m,n}(x,y)$] modes. For a cylindrical coordinate system, the solutions are the Laguerre-Gauss [$\mathrm{LG}_p^l(\rho,\phi)$] modes, which can present orbital angular momentum [36]. Therefore, a transverse DoF of light is associated to orbital angular momentum. In the first-order subspace, $\mathrm{LG}_0^{\pm 1}$ can be written as a linear combination of HG_{01} and HG_{10} [37]. Given the linear polarization basis $\{\hat{e_H}, \hat{e_V}\}$ and the first-order HG modes $\{\mathrm{HG}_{01}(x,y), \mathrm{HG}_{10}(x,y)\}$, the most general first-order spin-orbit mode can be written as [21]

$$\vec{E_{\mathrm{SO}}}(\vec{r}) = c_1\mathrm{HG}_{10}(x,y)\hat{e}_H + c_2\mathrm{HG}_{10}(x,y)\hat{e}_V + c_3\mathrm{HG}_{01}(x,y)\hat{e}_H + c_4\mathrm{HG}_{01}(x,y)\hat{e}_V, \quad (14)$$

where c_i are the complex numbers, with $i = 1, 2, 3$, and 4. Such a basis can be used for the quantization of the electromagnetic field. Denoting $\hat{e_H} \equiv H$, $\hat{e_V} \equiv V$, $\mathrm{HG}_{01}(\vec{r}) \equiv h$, and $\mathrm{HG}_{10}(\vec{r}) \equiv v$, the general quantum state of a photon can be written as

$$|\psi_{\mathrm{SO}}\rangle = a_{Hh}|Hh\rangle + a_{Hv}|Hv\rangle + a_{Vh}|Vh\rangle + a_{Vv}|Vv\rangle, \quad (15)$$

where a_{ij} is the probability amplitude of the normalized basis element $|ij\rangle$, with $i = H$ and V and $j = h$ and v. Equation (15) represents a general two-qubit state in DoF of polarization and transverse modes, with the computational basis defined as $\{|0\rangle = |H\rangle, |1\rangle = |V\rangle\}$ and $\{|0\rangle = |h\rangle, |1\rangle = |v\rangle\}$, respectively. For $a_{Hh} = a_{Vv} = 1/\sqrt{2}$ and $a_{Hv} = a_{Vh} = 0$, we have

$$|\Phi^+_{\mathrm{SO}}\rangle = \frac{1}{\sqrt{2}}(|Hh\rangle + |Vv\rangle), \quad (16)$$

which is a Bell state with maximal entanglement between internal DoF of a single photon (spin-orbit Bell state) [21]. For $a_{Hv} = a_{Vh} = 0$ and different arbitrary real a_{Hh} and a_{Vv}, we have a spin-orbit partially entangled state, as described in Eq. (11). To produce $|\Phi^+(p)\rangle$, which is an essential ingredient for preparation of ρ^{MDMS}, we need to coherently superpose the single-photon states $|Hh\rangle$ and $|Vv\rangle$ with different weights. It is important to stress that spin-orbit product states $|Hv\rangle = |01\rangle$ and $|Vh\rangle = |10\rangle$ [the needed states for the second part of the MDMS on the right-hand side of Eq. (10)] are not difficult to prepare. Then, if we have these three ingredients, we can perform an incoherent superposition controlling the population of each one in order to produce ρ^{MDMS}. We can obtain the incoherent superposition by using three independent single-photon sources to produce each one of the three required states.

We propose in Fig. 1(a) a linear optical circuit to produce ρ^{MDMS}. Let us start with a partially entangled state. A first single-photon source (SPS1) prepares a photon horizontally polarized ($|H\rangle$) with probability p^{I} [38]. A spatial light modulator (SLM) is used to prepare an HG transverse mode ($|h\rangle$). The photon state is then $|Hh\rangle$. A half-wave plate with an angle θ with respect the horizontal (HWP1@θ) produces the superposition

$$|Hh\rangle \longrightarrow \cos(2\theta)|Hh\rangle + \sin(2\theta)|Vh\rangle. \quad (17)$$

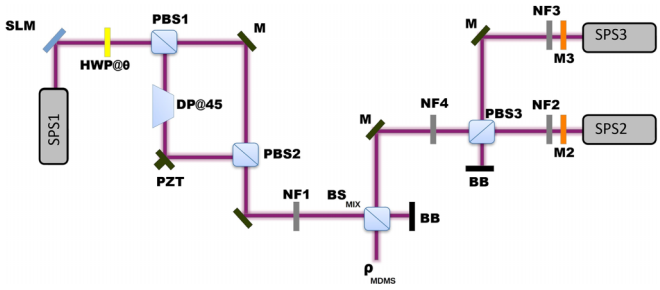

FIG. 1. Proposed optical circuit. SPS stands for single-photon source, SLM for spatial light modulator, HWP@θ for half-wave plates with fast axis performing an angle θ with the horizontal, PBS for polarizer beam splitters, DP@45 for Dove prism rotated by 45°, PZT for piezoelectric transducer, NF for neutral filter, M2 and M3 for holographic masks for preparation of the $\mathrm{HG}_{0,1}$ and $\mathrm{HG}_{1,0}$ modes, and M for mirrors.

This superposition enters in a Mach-Zehnder (MZ)-like interferometer mounted with two polarizer beam splitters (PBS) and two mirrors. The arm of the reflected incident beam in PBS1 (vertical polarization) has a Dove prism rotated by 45° with respect to the horizontal direction (DP@45°) in order to transform $|h\rangle \rightarrow |v\rangle$. The mirror of this arm is mounted in a piezoeletric ceramic transdutor (PZT) to control the phase difference with respect to the other arm of the interferometer. Both arms are recombined in PBS2 and we have the state

$$|\Phi(\theta)\rangle = \cos(2\theta)|Hh\rangle + e^{i\phi}\sin(2\theta)|Vv\rangle, \quad (18)$$

where ϕ is the difference of phase in the MZ interferometer. By setting $\phi = 2n\pi$, n as an integer, and $\sqrt{p} = \cos(2\theta)$, we recover the partially entangled state of Eq. (11). Note that if the SLM prepares the transverse photon state $|v\rangle$, we have a possibility to build an odd partially entangled state ($|\Psi^\pm\rangle = \cos(2\theta)|Hv\rangle \pm \sin(2\theta)|Vh\rangle$). The signal $\pm$ is set by ϕ [$2n\pi$ for $+$ and $(2n+1)\pi$ for $-$].

The output of the interferometer passes through a neutral filter (NF1) with amplitude transmission $t_1 = \sqrt{\epsilon}$ and will control the population of the state $|\Phi^+(\theta)\rangle$ in the spin-orbit DoF for ρ^{MDMS}. After NF1, the photon arrives at a balanced beam splitter (BS) responsible for the incoherent mixture ($\mathrm{BS}_{\mathrm{MIX}}$) that will transmit or reflect the photon with probability 1/2. The transmitted output of the $\mathrm{BS}_{\mathrm{MIX}}$ is blocked (BB) and only the reflected output is used. In the output of $\mathrm{BS}_{\mathrm{MIX}}$ we have $\epsilon|\Phi^+(\theta)\rangle\langle\Phi^+(\theta)|$ with probability $p^{\mathrm{I}}/2$.

To obtain the part of the product state in ρ^{MDMS}, we need to use a second independent single-photon source (SPS2) that produces a horizontally polarized photon state ($|H\rangle$) with probability p^{II}. This will be able to yield the product state $|Hv\rangle = |01\rangle$. We also need a third independent single-photon source (SPS3) that produces a photon vertically polarized ($|V\rangle$) with probability p^{III}. The holographic masks M2 and M3 will produce the transverse mode photon states $|v\rangle$ and $|h\rangle$, respectively. Then SPS2 (SPS3) will give rise to the state $|Hv\rangle = |01\rangle$ ($|Vh\rangle = |10\rangle$). The photon prepared by SPS2 passes through NF2, which has an amplitude transmission $t_2 = \sqrt{m}$, and will be transmitted by PBS3 with probability 1. On the other hand, the photon prepared by SPS3 passes through NF3, which has an amplitude transmission

$t_3 = \sqrt{1-m}$, and will be reflected in PBS3 with probability 1. Then, both photons pass through NF4, which is adjusted with the amplitude transmission $t_4 = \sqrt{1-\epsilon}$. After NF4 these photons are sent to BB_{MIX} and are transmitted with probability 1/2 each one. Then, from the contribution of the three SPS we have

$$\rho_{SO}^{MDMS} = \epsilon|\Phi^+(\theta)\rangle\langle\Phi^+(\theta)| + (1-\epsilon)[m|Hv\rangle\langle Hv| + (1-m)|Vh\rangle\langle Vh|, \quad (19)$$

with probability $p^I p^{II} p^{III}/8$.

In order to prepare a rank-2 state with $p = 1/2$, we need to set $\theta = 22.5^\circ$ and $m = 1$, leading to $t_2 = 1$ and $t_3 = 0$, yielding

$$\rho_{SO}^{(R2)} = \epsilon|\Phi_{SO}^+\rangle\langle\Phi_{SO}^+| + (1-\epsilon)|Hv\rangle\langle Hv|, \quad (20)$$

where $|\Phi_{SO}^+\rangle$ is given by Eq. (16).

In order to prepare a rank-3 state with $p = 1/2$, we need to set $\theta = 22.5^\circ$ to obtain

$$\rho_{SO}^{R3} = \epsilon|\Phi_{SO}^+\rangle\langle\Phi_{SO}^+| + (1-\epsilon)[m|Hv\rangle\langle Hv| + (1-m)|Vh\rangle\langle Vh|]. \quad (21)$$

In the next section we show the results for the simulation of these circuits and the QD calculations for each class of states.

IV. SIMULATIONS OF OPTICAL CIRCUITS

The MDMS preparation was proposed to be implemented through a linear optical circuit. In this case, the action of the optical elements composing the circuit over the spin-orbit photon state can be modeled by Jones matrix formalism [39]. For polarization states, the Jones matrices for the optical elements, such as HWP, PBS, and BS, are well known. For transverse modes, this is a nontrivial task. However, as we are limited to the first-order transverse modes (HG_{01} and HG_{10} modes), the analogy of this basis with the linear polarization basis $\{\hat{e_H}, \hat{e_V}\}$ is straightforward. Indeed, we can construct a Poincaré-like sphere for first-order transverse modes, where a first-order Laguerre-Gaussian beam plays the role of circular polarization [37]. Recently this powerful geometrical representation was extended for higher-order modes [40]. Then, we can represent a transverse mode state as a Jones vector and write unitary matrices for optical elements acting in the transverse mode. For example, the Jones matrix for a Dove prism acting on first-order HG modes is analogous to a HWP Jones matrix acting in the $\{\hat{e_H}, \hat{e_V}\}$ basis [32].

By using the Jones formalism, we construct a simulation of the optical circuit of Fig. 1 with MATLAB. Each Jones matrix for an optical element acts on the photon spin-orbit state accordingly. The resulting spin-orbit state is characterized by a two-qubit tomography for spin-orbit DoF, which is described in Ref. [32]. Once we obtain the density matrix, we can calculate the classical correlation (C), pairwise entanglement as measured by concurrence (C') [41], and QD (Q) as shown in Sec. II.

Let us now present the simulation results. Figure 2 exhibits the transverse density probability of photon detection that is related with the transverse profile the photon was prepared with. For rank-2 (R2) states, we have a pure state for $\epsilon = 0$ (product state) and $\epsilon = 1$ (spin-orbit entangled state). For intermediate ϵ values we have a mixed state with the mixing of the density probabilities. For rank-3 states (R3), we set $m = 1/4$. In this case, for $\epsilon = 0$ we have a mixed state of the two product states $|Hv\rangle$ and $|Vh\rangle$. Then, we have the prevalence of the $|Vh\rangle$ mode, given the chosen m. For $\epsilon = 1$, we also have a spin-orbit entangled state.

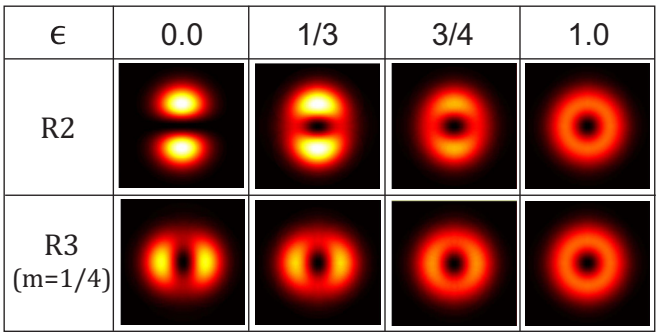

FIG. 2. Density probability of detection of a photon in the output transverse plane of the preparation circuit for different weights ϵ. The calculation was performed for rank-2 (R2) and rank-3 (R3) states. We used $m = 1/4$ for the rank-3 state.

The results for the correlations evaluated for R2 states are presented in Fig. 3 by setting $p = 0.5$. The circles dots are the results for the classical correlation C calculated as a function of ϵ. The dashed line is the theoretical prediction for the classical correlation C calculated as a function of ϵ. The squares are the results for the concurrence C' as a function of ϵ and the dotted line is the prediction of the concurrence by quantum theory. Finally, triangles dots are the results of quantum discord (Q) as a function of ϵ and the solid line is the

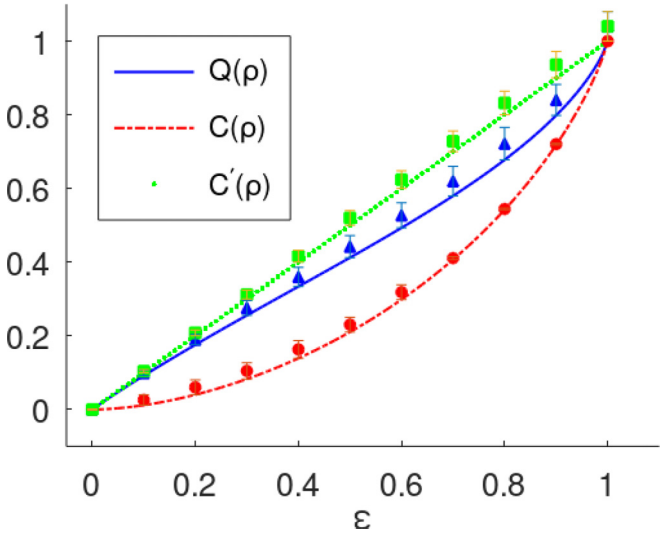

FIG. 3. Correlations for rank-2 states ($p = 0.5$) as a function of the weight ϵ. Dots are the results for the calculation from the state simulated by the preparation optical circuit using the Jones formalism. The lines are theoretical predictions of quantum theory. Classical correlation C: Circles dots and dashed line. Concurrence C': Squares dots and dotted line. Quantum discord Q: Triangles dots and solid line.

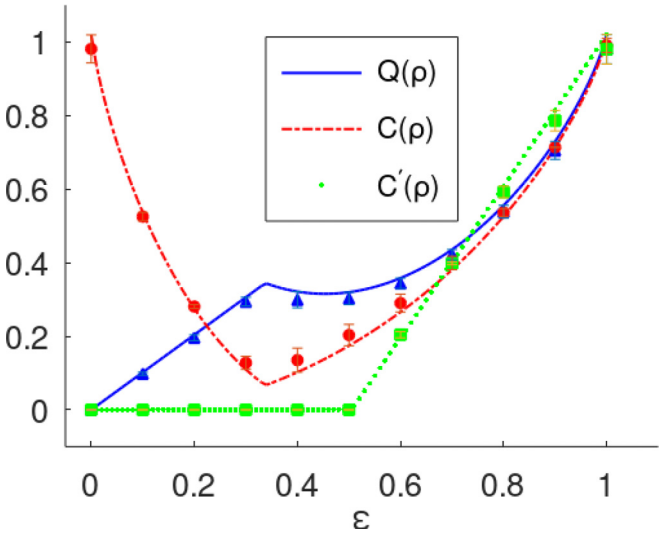

FIG. 4. Correlations for rank-3 states ($p = m = 0.5$) as function of the weight ϵ. Dots are the results for the calculation from the state simulated by the preparation optical circuit using the Jones formalism. The lines are theoretical predictions of quantum theory. Classical correlation C: Circles dots and dashed line. Concurrence C': Squares dots and dotted line. Quantum discord Q: Triangles dots and solid line.

discord predicted by quantum theory. The error bars were obtained by including typical realistic sources of noise of linear optical circuits through optical components such as half-wave plate angles ($\pm 1^\circ$) and transmission and reflection in beam splitters of the tomographic circuit ($R = 48\%$, $T = 49\%$). For this, we performed simulation varying the parameters in this error range and performed a statistical analysis of the results for different circuit runs, each with different sensitive parameters. As it can be seen, the error predicted for typical noise sources in optical devices is very small. In addition, it is worth stressing the very good agreement between the results calculated from the simulated state by the preparation circuit and the predictions of quantum theory for MDMS.

For $\epsilon = 0$ we have a product state and all correlations are vanishing, as expected. On the other hand, for $\epsilon = 1$, we have a maximally entangled Bell state and all correlations are equal to 1. Notice that all the correlations increase with ϵ being the concurrence dominant over QD and classical correlation.

The results for the R3 states are presented in Fig. 4 for $p = m = 0.5$. For this case, we have a mixing of a maximally entangled spin-orbit state and a balanced $|Hv\rangle$ and $|Vh\rangle$ product mixed state. As we can see, for ϵ from 0 to 0.5, the concurrence is vanishing but not QD. It is worth mentioning that, for $1/3 \leqslant \epsilon \leqslant 0.385$, we have found the minimal value for classical correlation and the local maximum for QD, which is the characteristic property of the MDMS. Again, the predicted errors for realistic optical devices are small and the agreement between the results for discord calculated from the simulated state by the preparation circuit and the predictions of quantum theory for MDMS is remarkable.

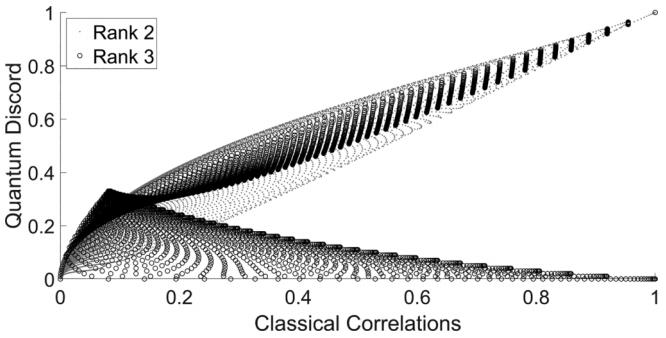

FIG. 5. Quantum discord versus classical correlation for a sample of rank-2 (gray dots) and rank-3 (black circles) states.

A global analysis can be performed by looking for QD as a function of the classical correlation, as shown in Fig. 5. The results were obtained by varying p in steps of 0.01. Gray dots are the results for R2 states [Eq. (19) for $m = 0$] and the black circles are the results for the R3 states [Eq. (19) for $m = 0$]. For a low value of the classical correlation, the QD for R3 states ($\theta = 22.5^\circ \rightarrow p = 1/2$, upper bound of black circles) is higher than the QD for R2 states ($\theta = 22.5^\circ \rightarrow p = 1/2$, upper bound of gray dots). On the other hand, when the classical correlation increases, R2 states present QD higher than that of R3 states. This result shows excellent agreement with the theoretical predictions presented in Ref. [10].

V. CONCLUSIONS

We have proposed an optical circuit to produce classes of rank-2 and rank-3 spin-orbit mixed states as well as others classes of mixed states, including MDMS. This optical circuit provides a useful tool to probe states with optimized quantum correlations for a fixed amount of classical correlation. Remarkably, for the case of rank-3 states, the circuit allows one to explore the optimization of quantum correlations (as measured by QD) in the absence of pairwise entanglement. The circuit has been simulated in a realistic experimental scenario, with the theoretical and simulated correlations showing excellent agreement. As a further development, we expect to provide an experimental realization of the circuit. This will allow for the explicit investigation (and control in certain cases) of decoherence as well as its impact on each kind of correlation. This is left for a future work.

ACKNOWLEDGMENTS

We are grateful for financial support from Conselho Nacional de Desenvolvimento Científico e Tecnológico (CNPq), Fundação Carlos Chagas Filho de Amparo à Pesquisa do Estado do Rio de Janeiro (FAPERJ), Coordenação de Aperfeiçoamento de Pessoal de Nível Superior - Brasil (CAPES) (Finance Code 001), and the Brazilian National Institute for Science and Technology of Quantum Information (CNPq INCT-IQ). W.F.B. acknowledges financial support from Grant No. H2020-FETOPEN and Grant PHOQUSING (GA No. 899544).

[1] M. A. Nielsen and I. L. Chuang, *Quantum Computation and Quantum Information* (Cambridge University, Cambridge, England, 2000).

[2] H. Ollivier and W. H. Zurek, Quantum Discord: A Measure of the Quantumness of Correlations, Phys. Rev. Lett. **88**, 017901 (2001).

[3] A. Brodutch, Discord and quantum computational resources, Phys. Rev. A **88**, 022307 (2013).

[4] Y. Huang, Scaling of quantum discord in spin models, Phys. Rev. B **89**, 054410 (2014).

[5] M. S. Sarandy, Classical correlation and quantum discord in critical systems, Phys. Rev. A **80**, 022108 (2009).

[6] K. Modi, H. Cable, M. Williamson, and V. Vedral, Quantum Correlations in Mixed-State Metrology, Phys. Rev. X **1**, 021022 (2011).

[7] Y. S. Abu-Mostafa, M. Magdon-Ismail, and H.-T. Lin, *Learning From Data* (AMLBook, 2012).

[8] B. Li, C.-L. Zhu, X.-B. Liang, B.-L. Ye, and S.-M. Fei, Quantum discord for multiqubit systems, Phys. Rev. A **104**, 012428 (2021).

[9] K. Bartkiewicz, K. Lemr, A. Černoch, and J. Soubusta, Measuring nonclassical correlations of two-photon states, Phys. Rev. A **87**, 062102 (2013).

[10] F. Galve, G. L. Giorgi, and R. Zambrini, Maximally discordant mixed states of two qubits, Phys. Rev. A **83**, 012102 (2011).

[11] X. X. Li, H. D. Yin, D. X. Li, and X. Q. Shao, Deterministic generation of maximally discordant mixed states by dissipation, Phys. Rev. A **101**, 012329 (2020).

[12] S. P. Walborn, A. N. de Oliveira, R. S. Thebaldi, and C. H. Monken, Entanglement and conservation of orbital angular momentum in spontaneous parametric down-conversion, Phys. Rev. A **69**, 023811 (2004).

[13] Q. Lin and B. He, Single-photon logic gates using minimal resources, Phys. Rev. A **80**, 042310 (2009).

[14] M. Hor-Meyll, D. S. Tasca, S. P. Walborn, P. H. Souto Ribeiro, M. M. Santos, and E. I. Duzzioni, Deterministic quantum computation with one photonic qubit, Phys. Rev. A **92**, 012337 (2015).

[15] J. T. Barreiro, T.-C. Wei, and P. G. Kwiat, Remote Preparation of Single-Photon "Hybrid" Entangled and Vector-Polarization States, Phys. Rev. Lett. **105**, 030407 (2010).

[16] V. D'Ambrosio, E. Nagali, S. P. Walborn, L. Aolita, S. Slussarenko, L. Marrucci, and F. Sciarrino, Complete experimental toolbox for alignment-free quantum communication, Nature (London) **3**, 961 (2012).

[17] E. Knill, R. Laflamme, and G. J. Milburn, A scheme for efficient quantum computation with linear optics, Nature (London) **409**, 46 (2001).

[18] N. Yoran and B. Reznik, Deterministic Linear Optics Quantum Computation with Single Photon Qubits, Phys. Rev. Lett. **91**, 037903 (2003).

[19] S. Popescu, Knill-Laflamme-Milburn Linear Optics Quantum Computation as a Measurement-Based Computation, Phys. Rev. Lett. **99**, 250501 (2007).

[20] P. Kok, W. J. Munro, K. Nemoto, T. C. Ralph, J. P. Dowling, and G. J. Milburn, Linear optical quantum computing with photonic qubits, Rev. Mod. Phys. **79**, 135 (2007).

[21] C. E. R. Souza, J. A. O. Huguenin, P. Milman, and A. Z. Khoury, Topological Phase for Spin-Orbit Transformations on a Laser Beam, Phys. Rev. Lett. **99**, 160401 (2007).

[22] C. V. S. Borges, M. Hor-Meyll, J. A. O. Huguenin, and A. Z. Khoury, Bell-like inequality for the spin-orbit separability of a laser beam, Phys. Rev. A **82**, 033833 (2010).

[23] X.-F. Qian, B. Little, J. C. Howell, and J. H. Eberly, Shifting the quantum-classical boundary: theory and experiment for statistically classical optical fields, Optica **2**, 611 (2015).

[24] T. Li, Q. Zeng, X. Song, and X. Zhang, Experimental contextuality in classical light, Scientifica **2017**, 1 (2017).

[25] M. H. M. Passos, W. F. Balthazar, J. A. de Barros, C. E. R. Souza, A. Z. Khoury, and J. A. O. Huguenin, Classical analog of quantum contextuality in spin-orbit laser modes, Phys. Rev. A **98**, 062116 (2018).

[26] W. F. Balthazar, C. E. R. Souza, D. P. Caetano, E. F. Galvão, J. A. O. Huguenin, and A. Z. Khoury, Tripartite nonseparability in classical optics, Opt. Lett. **41**, 5797 (2016).

[27] M. H. M. Passos, W. F. Balthazar, A. Z. Khoury, M. Hor-Meyll, L. Davidovich, and J. A. O. Huguenin, Experimental investigation of environment-induced entanglement using an all-optical setup, Phys. Rev. A **97**, 022321 (2018).

[28] C. E. R. Souza, C. V. S. Borges, A. Z. Khoury, J. A. O. Huguenin, L. Aolita, and S. P. Walborn, Quantum key distribution without a shared reference frame, Phys. Rev. A **77**, 032345 (2008).

[29] C. E. R. Souza and A. Z. Khoury, A Michelson controlled-not gate with a single-lens astigmatic mode converter, Opt. Express **18**, 9207 (2010).

[30] W. Balthazar, D. Caetano, C. Souza, and J. Huguenin, Using polarization to control the phase of spatial modes for application in quantum information, Braz. J. Phys. **44**, 658 (2014).

[31] W. F. Balthazar and J. A. O. Huguenin, Conditional operation using three degrees of freedom of a laser beam for application in quantum information, J. Opt. Soc. Am. B **33**, 1649 (2016).

[32] W. F. Balthazar, D. G. Braga, V. S. Lamego, M. H. M. Passos, and J. A. O. Huguenin, Spin-orbit x states, Phys. Rev. A **103**, 022411 (2021).

[33] S. Luo, Quantum discord for two-qubit systems, Phys. Rev. A **77**, 042303 (2008).

[34] D. Girolami and G. Adesso, Quantum discord for general two-qubit states: Analytical progress, Phys. Rev. A **83**, 052108 (2011).

[35] L. Henderson and V. Vedral, Classical, quantum and total correlations, J. Phys. A: Math. Gen. **34**, 6899 (2001).

[36] A. Siegman, *Lasers* (University Science, Sausalito, California, 1986).

[37] M. J. Padgett and J. Courtial, Poincaré-sphere equivalent for light beams containing orbital angular momentum, Opt. Lett. **24**, 430 (1999).

[38] A hyper-written index is used for the probability of photon production by a SPS.

[39] R. C. Jones, A new calculus for the treatment of optical systems. IV., J. Opt. Soc. Am. **32**, 486 (1942).

[40] Y. Shen, Z. Wang, X. Fu, D. Naidoo, and A. Forbes, SU(2) Poincaré sphere: A generalized representation for multidimensional structured light, Phys. Rev. A **102**, 031501(R) (2020).

[41] W. K. Wootters, Entanglement of Formation of an Arbitrary State of Two Qubits, Phys. Rev. Lett. **80**, 2245 (1998).